*Materials Science-Poland, 42(1), 2024, pp. 171-185*
*http://www.materialsscience.pwr.wroc.pl/*
*DOI: 10.2478/msp-2024-0011*

# Evaluation of cracking risk of 80MnSi8-6 nanobainitic steel during hot forging in the range of lower temperature limits

Paulina Lisiecka-Graca*, Łukasz Lisiecki, Krystian Zyguła, Marek Wojtaszek

AGH University of Krakow, Faculty of Metals Engineering and Industrial Computer Science, Mickiewicza 30 Ave., 30-059 Krakow, Poland

Nanobainitic steels exhibit an exceptional combination of high strength, good plasticity, impact toughness, and wear resistance. They are suitable for the production of large mass components through the open-die forging process. Subsequently, the forgings are air-cooled. An obstacle of this method is the extended time required for the large forgings to undergo a bainitic transformation, making the industrial implementation of this process economically unjustifiable. Nevertheless, nanobainitic steels also allow for the open-die forging of small batches of structural elements with high property requirements. A technological limitation lies in the necessity of performing a series of operations, leading to a prolonged processing time dependent on the shape of the product and the degree of deformation. Therefore, inter-operational reheating is often necessary, incurring costs and time consumption. This is particularly relevant to forgings with a mass ranging from a few to several dozen kilograms, which, due to their low thermal capacity, rapidly dissipate heat to the surroundings and tools. Designing an economical process with a limited number of reheating cycles requires advanced knowledge of material behavior under thermo-mechanical deformation parameters, including boundary conditions where a significant decrease in plasticity occurs and the risk of crack initiation. To obtain this information, a comprehensive analysis of the influence of thermo-mechanical parameters applied during the deformation of nanobainitic steel at relatively low temperatures on the flow characteristics and crack formation was conducted. To achieve this goal, the Digital Image Correlation method, the finite element method modeling considering damage criteria, and the macrostructural evaluation of deformed specimens were employed.

Keywords: *nanobainitic steels, multistage forging, microstructure, DIC – digital image correlation, finite element method (FEM) modeling, damage criteria*

## 1. Introduction

For many years, steel has been a fundamental structural material, primarily due to its well-established technological processes, characterized by high and stable physic-mechanical properties [1]. Among this group of materials, bainitic steels currently play a significant role. Bainite is a phase aggregate primarily composed of ferrite plates, with the presence of minority phases such as carbides or retained austenite [2]. This microstructure can be uniformly generated in large-scale forgings, such as steam turbines, or in selected areas of the product, for example, as a result of surface treatment leading to increased wear resistance [3]. Recent studies have indicated that comparing the mechanical properties of bainitic steels with those of conventional steels is favorable [4]. It has also been observed that the properties of this type of steel depend on the size of the phase components. The scale of bainite component sizes can be adjusted, ranging from hundreds of micrometers to tens of nanometers [5]. The change in the microstructure scale is reflected in properties that can be modified accordingly. A typical bainite microstructure consists of bainitic ferrite with a thickness of approximately 0.2–0.5 $\mu$m and an average length of about 100 $\mu$m [6]. Nanoscale microstructure, containing a mixture of very thin bainitic ferrite plates separated by carbon-enriched austenite, are the main characteristics of the so-called nanobainitic steel family [7]. Królicka et al. [8] demonstrated that the microstructure of nanobainitic steels significantly influences the properties of the manufactured products. Currently, steel manufacturers and users of steel products

* E-mail: graca@agh.edu.pl

have recognized the advantages resulting from obtaining this type of microstructure [9]. The most important benefit is the very favorable combination of strength and plasticity compared to many high-performance steels [10]. The presence of nanobainite is also associated with high wear resistance [11], as demonstrated by Du et al. [12] and Rios-Diez et al. [13]. Recent studies have shown that the combination of these properties may allow for the production of unconventional products from nanobainitic steel, such as armor for protection against projectiles [14]. Due to the high application potential of nanobainitic steels, they are currently the subject of intense research. The approach taken in these studies is that they must be cost-effective in production, which can be achieved by excluding expensive elements such as cobalt and nickel from their chemical composition. In this context, a high addition of aluminum is also unfavorable due to the purity requirements of ultra-high-strength steels. For these reasons, researchers have focused on developing an economical composition of elements, such as Fe-C-Si-Mn-Cr. Bainite subunits thinner than 100 nm are most commonly obtained through isothermal heat treatment in the temperature range of 200–400°C [4]. In the initial studies dedicated to the design of nanobainitic steels, the theory of bainitic phase transformation was employed, with the primary objective of achieving nanobainite at the lowest possible temperature. For this purpose, the chemical composition was selected to enable bainitic transformation at temperatures below 200°C. An example was the nanobainitic steel with the chemical composition Fe-0.78C-1.59Si-1.94Mn-1.33Cr-0.30Mo-0.02Ni-0.11V (wt.%), developed by Caballero et al. [15], subjected to the heat treatment at around 125 °C. The addition of approximately 2 wt. % of Si to the steel allowed the formation of a microstructure consisting of a mixture of bainitic ferrite, carbon-enriched retained austenite, and a certain amount of martensite. However, at the temperature of 125 °C, the transformation took more than two months, and it was possible to reduce this time to around 10 days with the temperature of 200 °C. The progression of research has led to a reduction in transformation time, and even finer bainitic microstructures were obtained at 200 °C in just three days [7]. An example is the steel with the chemical composition of Fe-0.83C-1.57Si-1.98Mn-1.02Cr-0.24Mo-1.54Co-0.11V. The proposed improvement was based on two solutions involving the control of austenitization conditions before bainitic transformation and the introduction of approximately 1.5 % of relatively expensive cobalt into the chemical composition. This approach accelerated the kinetics of the transformation. As a result, the obtained material exhibited a very good combination of yield strength, ultimate tensile strength, ductility, and respectable levels of fracture [16]. In the research on the production of nanobainitic steel conducted by Garcia-Mateo et al. [17], economic aspects were taken into account. The goal was to obtain new nanostructural steels through transformation at low temperatures within an industrially acceptable time and using inexpensive alloying additions. On the other hand, studies conducted by Wojtaszek et al. [18] showed that an example of a steel that, under carefully developed conditions, can meet these criteria is 80MnSi8-6 steel. The authors focused on developing favorable combinations of thermo-mechanical forging parameters of the investigated steel. Understanding these parameters is a key condition for obtaining forgings with a microstructure suitable for nanobainitic transformation in the subsequent stage. They also demonstrated that their proposed method based on integrated modeling is useful in designing shaping processes for this material using prolonged processes that require multiple operations. An example of this is multi-stage open-die forging on presses with low strain rates.

Due to the favorable combination of strength, plasticity, and utility properties, nanobainitic steels are suitable for the production of highly responsible structural elements with medium to large masses. Such products are manufactured using open-die forging operations, followed by air cooling of the forgings. A limitation of the technology is the fact that the hardening time for large forgings to achieve a uniform bainitic microstructure is counted in days. Therefore, the process is currently economically impractical. Additionally, industrial heat treatment facilities are designed to handle procedures lasting up to about 4 hours, not for 20 hours or more [19]. On the other hand, using nanobainitic steel, it is possible to forge small batches of structural elements with significantly smaller dimensions, such as crankshafts, rolls, rings, or sleeves. This is especially relevant for structural elements intended to operate in conditions where the mechanism of damage may be wear-related [20].

However, it should be noted that a limitation of open-die forging technology is the need to apply a series of operations, which requires a correspondingly long time. This time depends on the adopted deformation and the final shape of the forging. As a result, inter-operational reheating is often necessary, which is costly, time-consuming, and leads to grain growth. This is especially true for forgings with a mass ranging from a few to several dozen kilograms, which, due to their low thermal capacity, rapidly dissipate heat to the surroundings and tools [18]. Therefore, the manufacturing technology for such products needs to be developed in a way that minimizes the number of heat treatments. This approach aligns with the global trend favoring technological solutions that reduce energy consumption [21]. However, in some cases, this approach requires continuing the forging process at relatively low temperatures. During hot forging, the decrease in temperature to a critical value at a given strain rate can occur only in a part of the forging, for example, in the contact zone with a cooler tool. This condition may lead to the occurrence of defects in this area, disqualifying the forging as a fully valid product.

Therefore, designing a multi-stage forging technology for nanobainitic steels requires knowledge of the material's behavior over a wide range of thermo-mechanical deformation parameters. While information on the standard range of hot forging is available in the literature, including [18], there is a lack of data on the limiting values of forging parameters. This is especially true for combinations of temperature and strain rate where a significant decrease in plasticity occurs, setting the conditions for forging defects and even material failure. The limits of these parameters can be determined by analyzing the influence of deformation parameters at relatively low temperatures on the flow characteristics and the mechanism of potential crack formation. For this purpose, numerical methods such as finite element method (FEM) analysis conducted with a properly selected damage criterion and macrostructure analysis of samples in a deformed state can be applied. However, excellent results can be achieved using the non-contact optical technique of digital image correlation (DIC), which involves measuring displacements and deformations in real-time. The DIC test results allow for recording and analyzing material flow under the chosen conditions, including determining whether material integrity is compromised. The application of this research technique, especially in combination with FEM modeling and damage criterion analysis, allows us to determine the limits of forging parameters with high accuracy.

The DIC technique is increasingly being used to assess the plasticity of materials subjected to deformation in compression, tension, torsion, bending, and under complex loading conditions. For precise deformation analysis, the international standard ISO 12004-2:2021 recommends using a stereophonic DIC system, as two-dimensional (2D) DIC systems may not provide accurate deformation representation due to errors associated with out-of-plane motion and deformation [22]. The results obtained in this way are easily comparable with the outcomes of numerical analyses and can be used for their verification. Therefore, the DIC method is widely applied to evaluate the behavior of metals and alloys during deformation under various conditions. An interesting approach to this issue was presented by Szalai et al. [23], who used a DIC system to assess the effectiveness of lubricants and polytetrafluoroethylene (PTFE) films applied during the deformation of thin aluminum sheets manufactured for the electronic and automotive industries. In another study [24], this measurement technique was applied to accurately determine the thermo-mechanical properties of the age-hardenable Inconel 718 alloy. In the work of Van der Heijde et al. [25], the focus was on assessing the influence of sample thickness on the occurrence of the Lüders effect in hot-rolled AISI 1524 steel. The results obtained using the DIC method allowed them to suggest that Lüders bands have a three-dimensional character and demonstrate that their specific features depend on the dimensions of the loaded structure.

In the study [26], the influence of welds on the deformability of high-strength 3rd GEN AHSS steel was investigated, with particular attention to the location of the initiation of cracking. The results obtained using the DIC system were complemented with FEM modeling outcomes. Another example of combining DIC and FEM modeling methods was presented in the work of He et al. [27], where a method using the capabilities of full-field digital image correlation was applied for the simultaneous evaluation of multiple stress-strain relationships for fiber-reinforced composites. The results obtained in this way were correlated with the outcomes of numerical modeling. On the other hand, Roux et al. [28] focused on determining ductile damage model parameters for the Lemaitre damage model. There are numerous examples demonstrating the usefulness of the DIC technique for broadly defined deformability analysis.

The analysis of the state of the art based on the relevant literature has demonstrated that the DIC technique is currently a widely used and extremely useful tool for analyzing the deformability of steels and alloys. At the same time, it has been noted that there is a lack of comprehensive information regarding the lower boundary thermal parameters during the forging of the investigated 80MnSi8-6 steel. This observation served as motivation for conducting the research, the results of which are compiled in this paper.

# 2. Material and motivation

## 2.1. Initial material

The research's initial material was 80MnSi8-6 steel, obtained through casting processes and subsequently subjected to initial hot forging to achieve microstructure homogenization and the required quality. The chemical composition of the steel in its as-delivered state is presented in Table 1, and a microstructure image is shown in Figure 1.

Table 1. Chemical composition of 80MnSi8-6 steel [%wt.]

| Element | C | Si | Mn | P | S | Cr | Mo | V | Fe |
|---|---|---|---|---|---|---|---|---|---|
| Content, mass % | 0.79 | 1.55 | 1.9 | 0.003 | 0.003 | 1.3 | 0.25 | 0.11 | Bal. |

The microstructure presented in Figure 1 is characterized by a complex structure composed of ferrite grains (bright areas), regions of pearlite (clearly visible as alternating plates of ferrite and cementite), and bainite (dark areas with a lath-like structure). The ferrite exhibits varying morphology, with both smaller, regular-shaped grains and larger, irregular-shaped grains observable.

## 2.2. Motivation

During the research, several assumptions were adopted. In the case of the 80MnSi8-6 steel selected for the study, the hot forming temperature range lies above 900°C. However, in the case of multi-stage forging, the production of the workpiece requires a long time, depending on the forging strategy, the degree of deformation, and the shape of the forging. As a result, inter-operational reheating is often necessary, which is costly, time-consuming, and leads to unfavorable changes in the microstructure. This is particularly true for forgings with a mass ranging from a few to several dozen kilograms, which have low thermal capacity and rapidly dissipate heat to the surroundings and tools. The forging strategy for such products can be developed to minimize the number of heat treatments to the necessary minimum. However, continuing forging during the time of inter-operational reheating poses a risk of a significant decrease in temperature in parts of the forging, for example, in the contact zone with a cooler tool. In such cases, it is crucial to understand the combinations of lower temperature and strain rates that must not be exceeded due to the risk of defects or material failure. To address this, tests with DIC measurements and FEM modeling considering damage criteria were employed as suitable tools for this purpose.

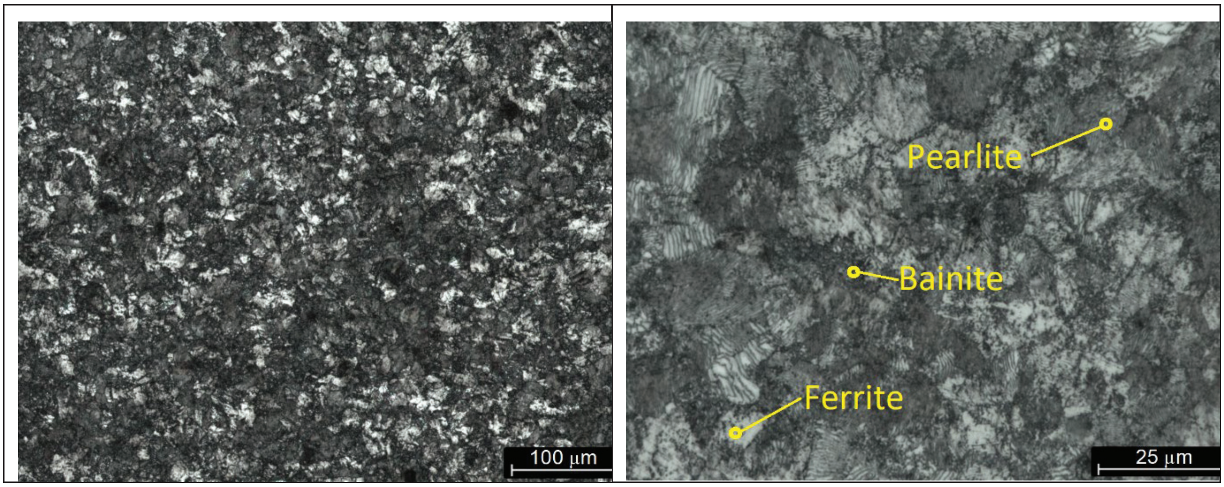


Fig. 1. Microstructure of 80MnSi8-6 steel in delivery condition

## 3. Experimental procedure

The compression tests were conducted on a hydraulic press with a maximum force of 5000 kN. To analyze the distribution of displacements and deformations on the sample surface during the tests, a DIC Q-400 system was employed (Fig. 2) [28–30]. The basic parameters of the system, along with the calibration plates used, are presented in Table 2. In this method, a stochastic pattern is painted on the specimen to determine the displacement of objects through image correlation analysis. Before starting the heating process, the samples were coated with matte, black fire-resistant paint, and white stochastic speckles were applied using boron nitride. Measurements were performed on the external surface of the sample. The correlation algorithm compares the positions of individual speckles on successive images with respect to the reference image and then calculates the change in position in two axes (Δx; Δy). Based on this, displacement and strain quantities are computed.

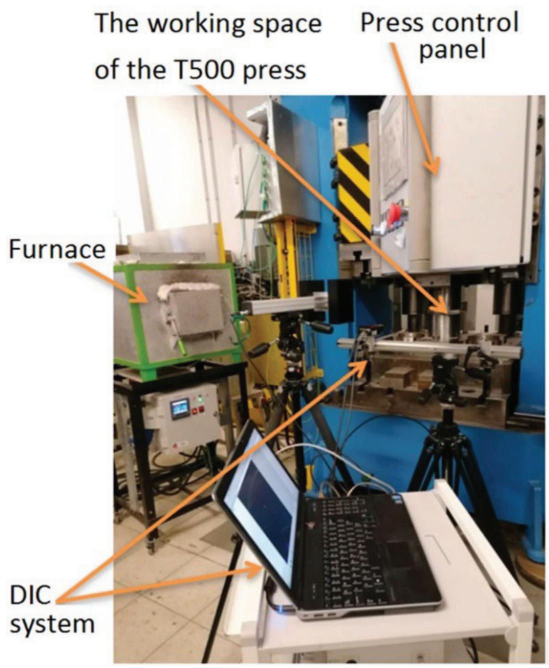


Fig. 2. Test stand with main equipment

Specimens with a diameter of 20 mm and a height of 40 mm were prepared to perform the tests. Compression tests with DIC analysis were conducted at temperatures of 600, 700, and 900°C and at traverse velocities of 1 and 10 mm·s$^{-1}$. The goal was to identify, for the investigated steel, the temperatures that are critical for the adopted tool velocity during forging in industrial conditions. This means that deformation tests under conditions where a temperature decreases below these values in any material zone will result in defects and a significant risk of material failure. For samples with a diameter of 20 mm arranged in a lateral position, the adopted traverse velocity reflects the typical deformation velocity ranges for open-die forging on hydraulic presses. The variants of the

Table 2. DIC Q-400 system parameters [31]

| System components | System parameters | | |
|---|---|---|---|
| Cameras | | Max resolution | 5 MPx 2448 x 2050 pixel |
| | | Pixel size | 3.45 $\mu$m x 3.45 $\mu$m |
| | | Shutter time | 4 $\mu$sec- 2 sec |
| Objectives | 1.9/35 | Focal length | 34.9 mm |
| | | Focal distance (F-number) | 1.9 |
| Light source | | Monochromatic | |
| | | Wavelength | Red (620-750nm) |
| Calibration plates | GI-06-WMB | 9x9 | Object size 60 mm |

samples, along with the assumed temperatures and deformation velocity, are presented in Table 3.

Compression tests at temperatures of 600–900°C were performed to examine the behavior of the material and its susceptibility to fracture at extremely low hot forging temperatures. This range was determined based on the results of open-die forging simulations of forging with a variable diameter along its cross-section. Despite observing the temperature regime for a given material of 950–1250°C, the occurrence of areas with a much lower temperature was observed (Fig. 3a). These areas occurred during the forming of the forging neck and were caused by long-term contact of the material with the tool. Additionally, the material in this area was deformed very intensively, as evidenced by high values of effective stress (Fig. 3b) and plastic strain (Fig. 3c). These factors could have resulted in damage to the forging in this area during the forging process.

In the next stage, numerical modeling of all adopted test variants was carried out. Compression process simulations were conducted using the FEM with the QForm UK software. During the modeling, the material was considered as an incompressible, isotropic continuum. The range of elastic deformations was not taken into account. The program performed calculations based on a rigid-viscoplastic model with strain-rate dependency, where the flow stress depends on the magnitude of deformation, strain rate, and temperature. The calculations incorporated heat generation during plastic deformation. The first law of Levanov was used to describe friction. To represent material rheology, flow curves were introduced into the QForm software, developed based on plastometric tests and thermal characteristics of materials. The data necessary for correct modeling of the compression test of 80MnSi8-6 steel were derived from our own research, the results of which are presented in the work [18].

A plastic model of the deformed material and a rigid tool model were used in the numerical simulation of the forging process and compression test. The stress-strain curve during compression of an axisymmetric sample at a temperature of 600°C is shown in Figure 4a. The machine parameters were transferred from the laboratory process. The nominal velocity of the working tool depended on the test variant: 1 mm/s or 10 mm/s. The maximum load was 5MN. The relationship between the velocity change and the load is shown in Figure 4b. Friction conditions were assumed at the boundary of the deformed material and the tool according to the Levanov model, taking into account a friction factor of 0.8 and a Levanov coefficient of 1.25. Heat transfer in this area was characterized by a heat transfer coefficient of 50 000 W/(m$^2$K). The adopted ambient conditions included a temperature of 20°C, an emissivity of 0.6, and a heat exchange coefficient with the environment of 30 W/(m$^2$K). The cooling time of the material in the air during transport from the furnace to the press was also assumed to be 5 s and the cooling time in the tools was 3 s.

The microstructure of the as-delivered steel was assessed using optical microscopy on a Leica DM4000M light microscope. The sample was embedded in epoxy resin, ground, polished, and etched in a 5 % solution of nitric acid in alcohol.

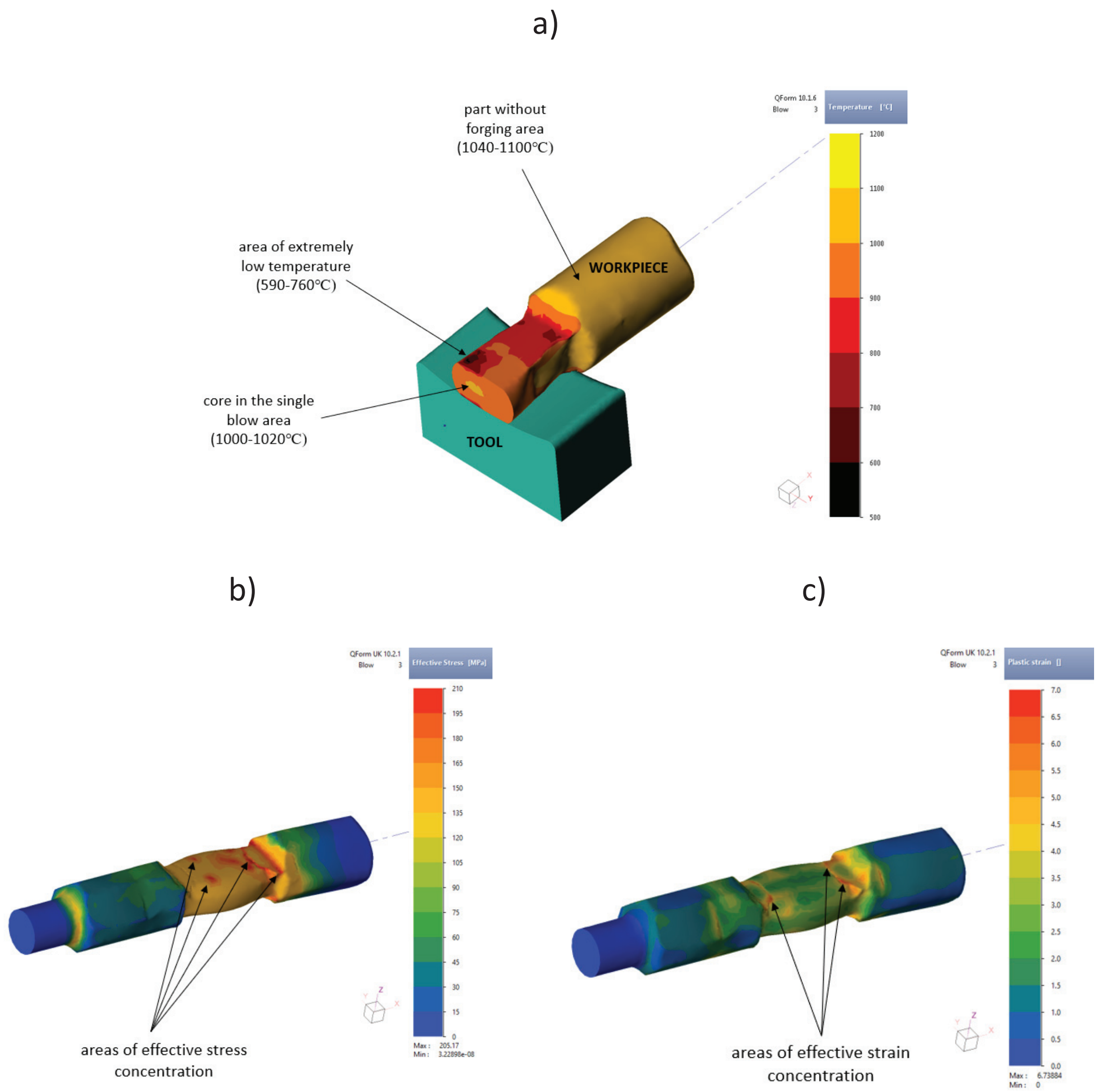


Fig. 3. Results of numerical simulation of open-die forging process: a) temperature distribution in the material, including localization of the area of low temperature range; b) effective stress distribution; c) plastic strain distribution

# 4. Results and discussion

Research on the deformability of 80MnSi8-6 steel was conducted in two stages. In the first stage, three different forging temperatures and two traverse velocities were adopted, as shown in Table 3. The table also includes labeling used to describe the samples.

Figure 5 shows microstructure images of samples after DIC tests conducted at a temperature of 600°C and at different values of the linear velocity of the upper tool, specifically 1 and 10 mm/s. The microstructure of the samples subjected to compression in the lateral position between flat tools during the tests is strongly oriented, regardless of the applied linear velocity of the tool. The direction of grain deformation coincides with the direction of material flow during deformation. The banded arrangement of microstructure components is particularly visible in the case of samples observed at

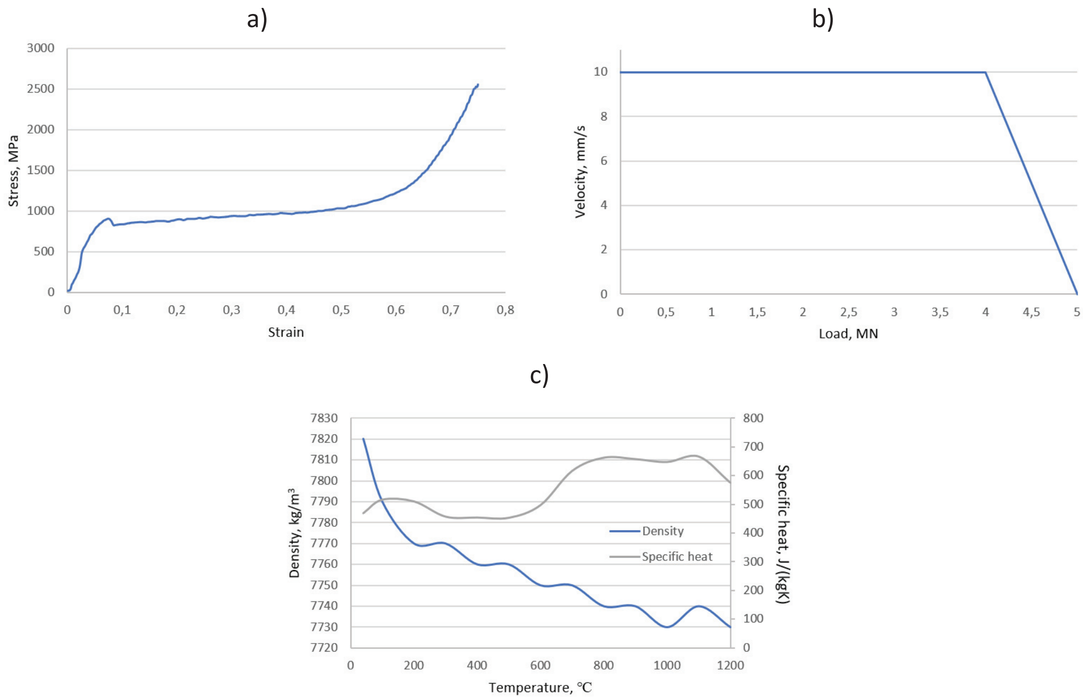


Fig. 4. Examples of dependencies used in numerical simulation: a) stress-strain curve in 600, b) hydraulic press characteristic, c) changes of density and specific heat of the material depending on the temperature

Table 3. Effect of deformation process parameters on specimen condition

| Sample labeling | Temperature, °C | Traverse velocity, mm/s | Crack |
|---|---|---|---|
| P1_600 | 600 | 1 | No |
| P2_600 | 600 | 10 | Yes |
| P3_700 | 700 | 1 | No |
| P4_700 | 700 | 10 | No |
| P5_900 | 900 | 1 | No |

higher magnification after deformation at a higher velocity of 10 mm/s (Fig. 5d). Such strong deformation and orientation occurring at higher DIC test velocity could have been the direct cause of coherence failure and crack formation. Individual microstructure components are quite regularly distributed. Bright ferrite grains, dark areas corresponding to bainite, and perlite plates are arranged in bands oriented perpendicular to the direction of force application. The bainitic ferrite component within the bainite is predominantly present in the form of very fine plates.

At this stage of the research, the results obtained from DIC measurements were compared with the numerical simulation results from FEM. The state of the samples after deformation in the macro-scale was also evaluated. Surface cracks were observed on the sample deformed at a temperature of 600°C with a velocity of 10 mm/s (Fig. 5e). However, in the case of the other samples deformed under the conditions listed in Table 3, no defects, including cracks or discontinuities formed during deformation, were observed on their surfaces.

The strain distribution recorded by the DIC system during the compression test of sample P4_700 (Fig. 6) showed significant localization of deformation in the central part of the sample. A satisfactory agreement was also observed between the results of the digital image correlation analysis and the FEM modeling results. Similar results of agreement were obtained for the other analyzed samples. Based on these observations, it can be inferred that the boundary conditions and the choice of the model adopted during the design of the numerical analysis were correctly determined.

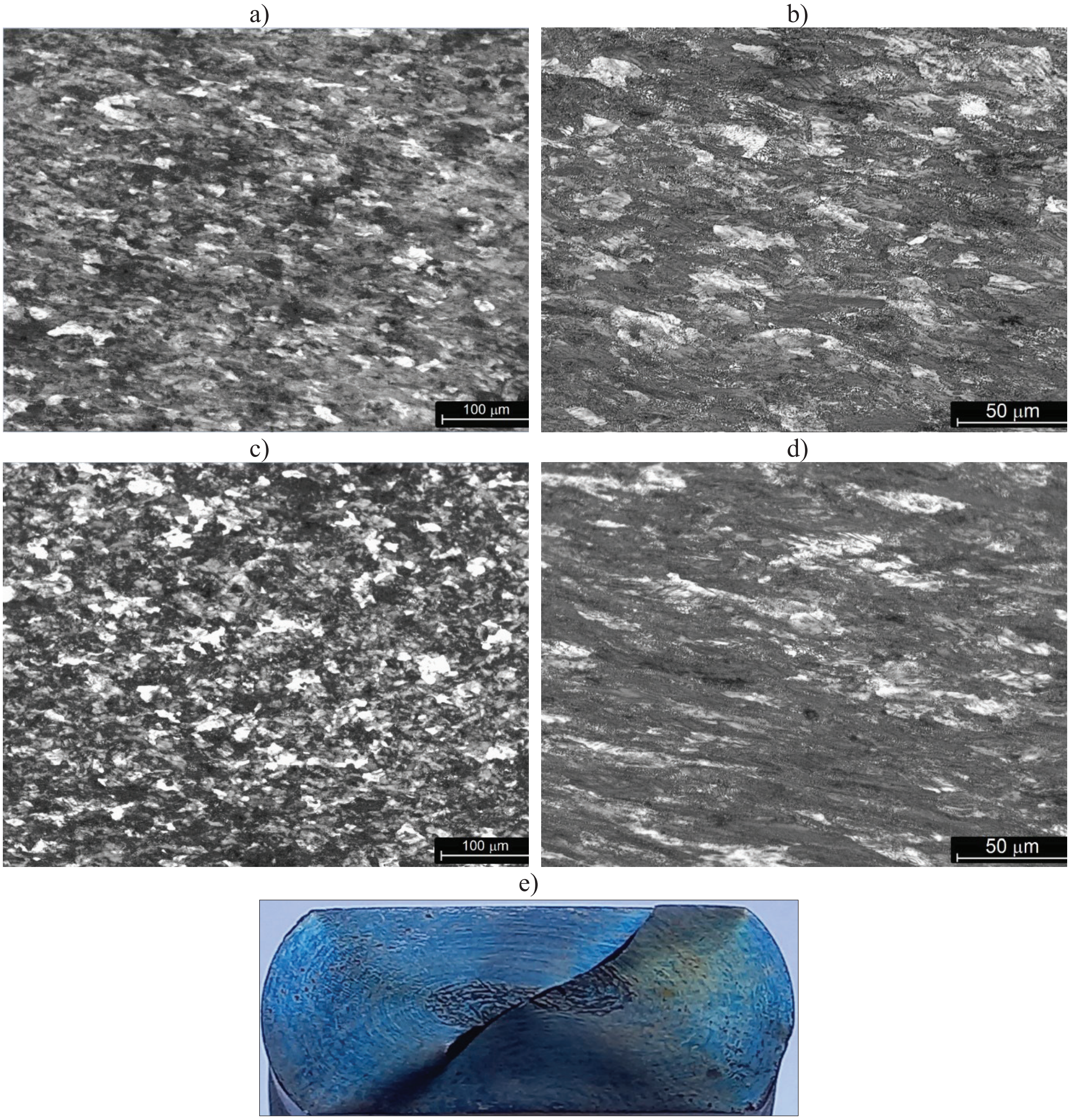


Fig. 5. The microstructure of samples P1_600 – a), b); P2_600 – c), d) and macrostructure of the cracking area in sample P2_600

The results obtained in the first stage of the study and their analysis allowed limiting the temperature range for material forming, where the risk of cracking during forging is most significant. It was observed that this range falls within the temperature range between 600 and 700°C. To determine the influence of the applied velocity during the test in the adopted temperature range on the tendency for cracking, three traverse velocities of the press were applied: 1.0, 5.0, and 10 mm/s.

In Fig. 7, a comparison of the strain distribution maps obtained from the DIC system and based on numerical FEM simulation is presented, along with the force changes during the test for all analyzed samples. The greatest differences in strain values were obtained for the sample deformed at a velocity of 5 mm/s and at a temperature of 600°C. Additionally, in this case, the largest differences in the results of force changes over time between numerical simulation and data obtained from the

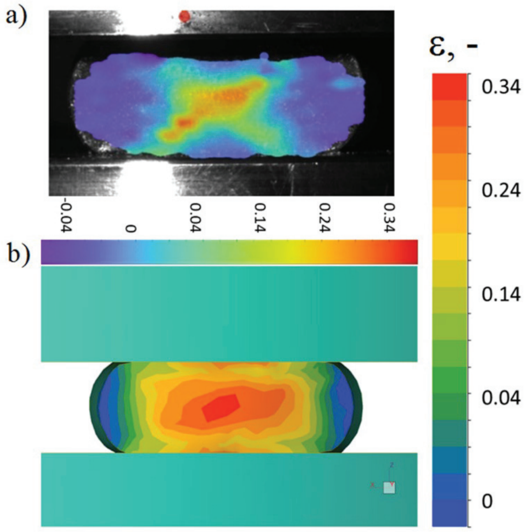


Fig. 6. Distribution of true principal strain ($\varepsilon$) during compression of sample P4_700 of 80MnSi8-6 steel obtained by methods: a) digital image correlation using DIC Q400 system with Istra4D software, and b) numerical FEM modeling with QForm software

machine were observed. This difference is approximately 23 %. This may be due to the fact that for the given deformation conditions, the highest risk of crack formation was determined (Table 4). For the remaining samples, both strain distribution maps and the change in force over time were determined based on numerical simulation were consistent with the data obtained during the tests. The difference between the registered force values and those determined based on numerical simulation for the other samples is approximately 6%.

The next step involved estimating the risk of material damage at reduced temperatures during hot forging. For this purpose, numerical FEM modeling was applied, incorporating an additional damage criterion. The Cockroft-Latham criterion [32] was selected as the most favorable, commonly used, for analyzing the material's ability to maintain integrity in plastic deformation processes. The Cockroft-Latham criterion is described by the equation:

$$\int_0^{\overline{\varepsilon}_f} \sigma_1 d\overline{\varepsilon} = C_1 \tag{1}$$

Table 4. Maximum damage criterion value determined for individual samples

| Sample | Temperature, °C | Velocity, mm/s | Cockrofta – Lathama criterion |
|---|---|---|---|
| P600_1 | 600 | 1 | 306 |
| P600_5 | | 5 | **267** |
| P600_10 | | 10 | 367 |
| P700_1 | 700 | 1 | 297 |
| P700_5 | | 5 | **268** |
| P700_10 | | 10 | 360 |

where: $\sigma_1$ is the largest principal stress, and $\overline{\varepsilon}$ is the effective plastic strain.

In the adopted criterion, the value of the maximum principal stress is integrated. This criterion is based on the accumulation of a damage indicator when the value of the maximum principal stress is greater than zero. This means that in certain cases, the risk may increase even when the values of the average stress are less than zero. This has significant implications in forging processes, where we mainly deal with negative values of average stress. The obtained results are presented in Fig. 8. The distribution of the Cockroft-Latham criterion clearly indicates the central part of the sample as the area of potential crack initiation, corresponding to the previously recorded (using the DIC system) maximum strain values.

The deformed samples in all adopted variants were analyzed. Based on the obtained results, the maximum values of the cracking criterion were determined, and then the critical value of temperature and traverse velocity for the selected material was determined. The results are presented in Table 4.

Analyzing the obtained results, it was observed that for samples deformed at a velocity of 5 mm/s, the value of the Cockroft-Latham criterion is the lowest. This indicates that the use of this velocity guarantees the lowest risk of cracking for the tested steel. On the other hand, the highest risk was recorded for the sample deformed at a velocity of 10 mm/s at 600°C. Additionally, it is worth noting that the difference in the size of the cracking criterion recorded at a velocity of 5 mm/s for the

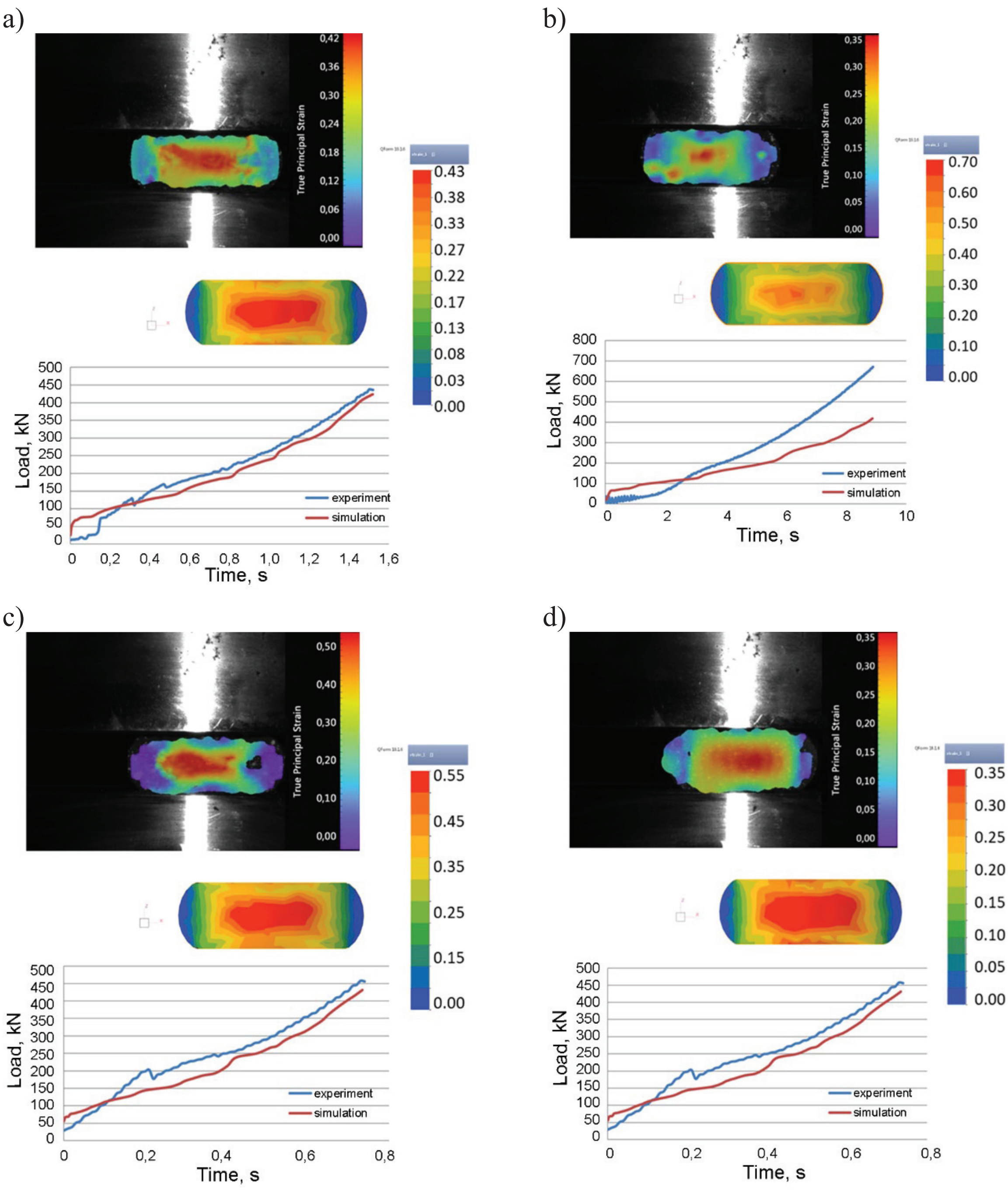


Fig. 7. Contined

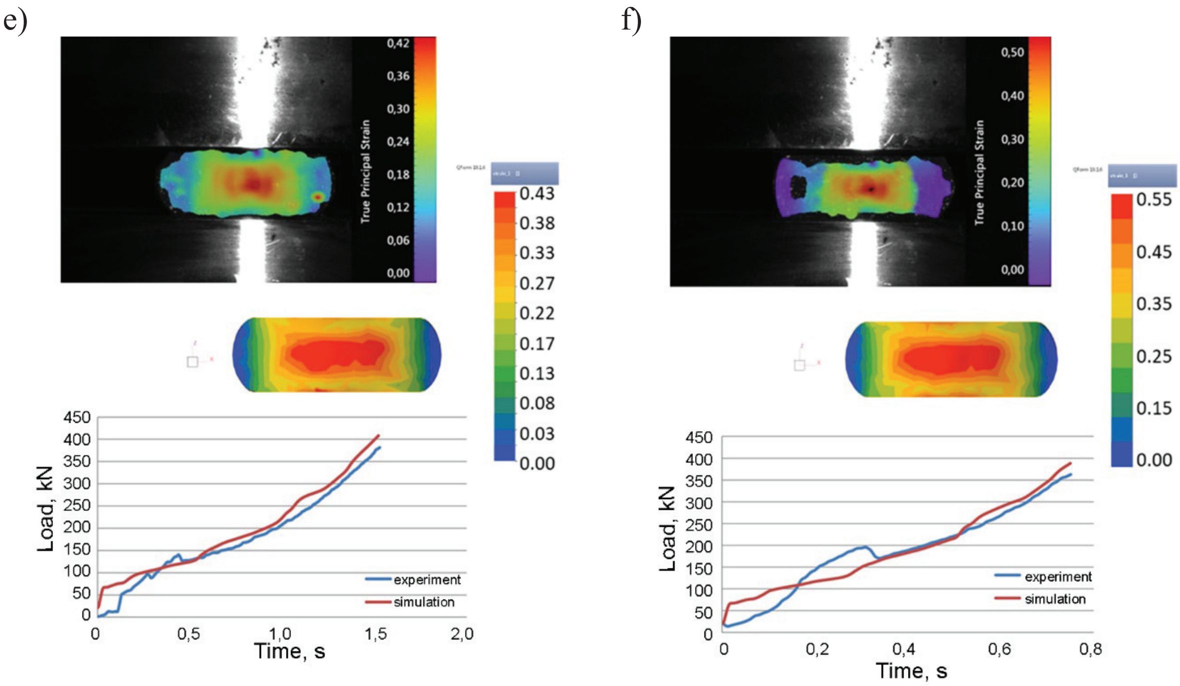


Fig. 7. The strain distribution maps obtained from measurements with the DIC system and based on numerical simulation results, together with force changes over time obtained from FEM simulation and direct measurement on the press for specimens deformed at 600°C and 700°C: P600_1 – a), P600_5 – b), P600_10 – c), P700_1 – d), P700_5 – e), P700_10 – f)

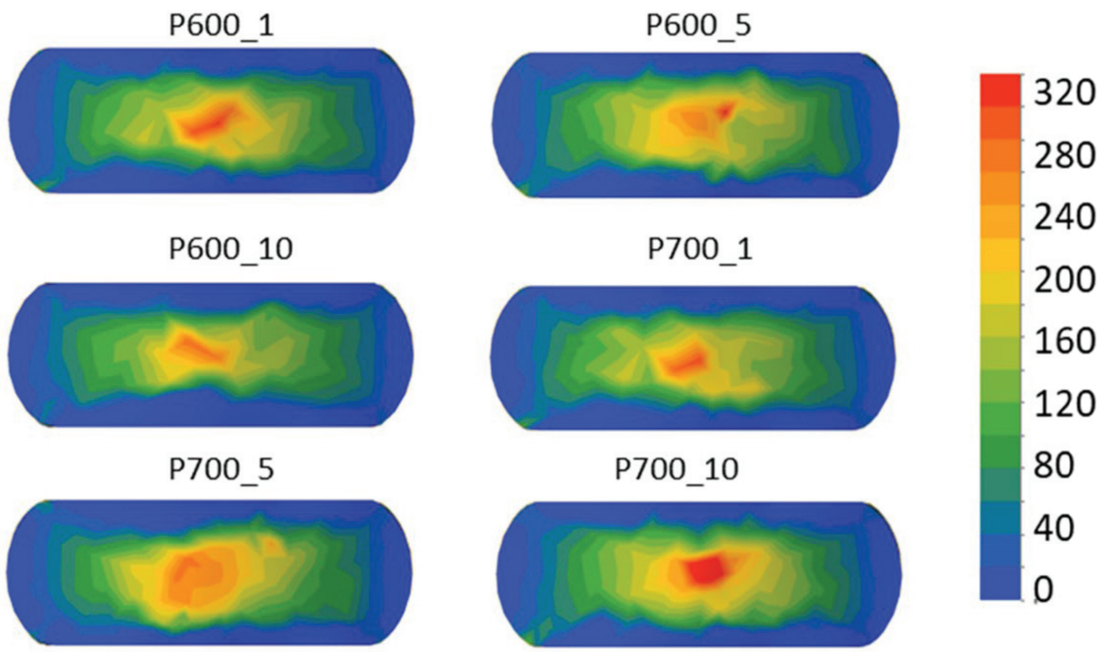


Fig. 8. Summary of FEM modeling results, including the distribution of the damage parameter according to the Cockcroft-Latham damage criterion for the analyzed variants of the compression test

sample deformed at 600°C and 700°C is negligible, indicating the possibility of using a lower forging temperature at this velocity, with a slight increase in the risk of material cracking. The fracture criterion value for the sample with a crack (temperature: 600°C, working tool movement velocity: 10 mm/s) was 366.9. This value is 20% higher than the maximum criterion value achieved for a sample deformed at a lower velocity (1 mm/s) at the same temperature.

## 5. Conclusions

Based on the results of the risk assessment for cracking in 80MnSi8-6 steel during hot forging at lower temperature limits and their analysis, the following conclusions can be drawn:

1. The distributions of strain values determined based on parameters obtained during tests and the critical strain values determined using the digital image correlation (DIC) system allowed for the assessment of the deformability of 80MnSi8-6 steel during hot forging.
2. Preliminary studies allowed us to narrow down the temperature range at which there is the highest risk of crack formation during the deformation process to values between 600 and 700°C.
3. Distributions of the damage parameter values were determined according to the Cockcroft-Latham criterion. Based on these distributions, it was possible to identify the ranges of traverse velocity and temperature necessary to maintain the material without damage during the deformation process. It was also noted that within the determined temperature range, the optimal traverse velocity is crucial, and for the analyzed material, it was 5 mm/s.
4. The results of the conducted research can be used in the numerical analysis of hot deformation processes for products made of the examined steel, such as the multi-stage open-die forging process in laboratory or industrial conditions. This approach will help identify those areas that are particularly prone to cracking during deformation and avoid parameter combinations that may cause such an effect. This is crucial during deformation at relatively low temperatures, especially in cases of local temperature decreases, for example, in the contact zone of the forging with a cooler tool.

The presented research, along with the free forging process, was conducted under laboratory conditions, where it is possible to limit the influence of certain factors, such as the variation in tool temperature between sequential series of produced forgings. The next stage of the research will involve consideration of additional dependencies raised from the nature of serial forging production and transferring the proposed procedure into the industrial conditions.

### Acknowledgement

This study was funded by the National Science Centre, Poland under "M-ERA.NET 2 Call 2020", Grant No. 2020/02/Y/ST8/00107.

### References

[1] Kowalczyk K, Jabłońska M, Rusz S, Junak G. Influence of recrystallization annealing on the properties and structure of low-carbon ferritic steel IF. *Arch Metall Mater* 2018; 63(4): 1957–61. doi:10.24425/amm.2018.125130.

[2] Bhadeshia HKDH. Atomic mechanism of the bainite transformation. *J Heat Treatm Mat.* 2017; 72(6): 340–345. doi:10.3139/105.110338.

[3] Zhang FC, Wang TS, Zhang P, Zhang CL, Lv B, Zhang M, Zhang YZ. A novel method for the development of a low-temperature bainitic microstructure in the surface layer of low-carbon steel. *Scr Mater* 2008; 59: 294–296. doi:10.1016/j.scriptamat.2008.03.024.

[4] Królicka A, Żak A, Kuziak R, Radwański K, Ambroziak A. Decomposition mechanisms of continuously cooled bainitic rail in the critical heat-affected zone of a flash-butt welded joints. *Mater Sci-Pol* 2021; 39(4): 615–25. doi:10.2478/msp-2022-0002.

[5] Zhu Z, Han J, Li H, Lu C. High temperature processed high Nb X80 steel with excellent heat-affected zone toughness. *Mater Lett* 2016; 163: 171–174. doi:10.1016/j.matlet.2015.10.071.

[6] Avishan B, Talebi P, Tekeli S, Yazdani S. Producing nanobainite on carburized surface of a low-carbon low-alloy steel. *JMEPEG* 2023; 32: 211–220. doi:10.1007/s11665-022-07096-6.

[7] Garcia-Mateo C, Caballero FG, Sourmail T, Smanio V, Garcia de Andres C. Industrialised nanocrystalline bainitic steels. Design approach. *Int J Mater Res* 2014; 105(8): 725–734. doi:10.3139/146.111090.

[8] Królicka A, Janik A, Żak A, Radwański K. The qualitative–quantitative approach to microstructural characterization of nanostructured bainitic steels using electron microscopy methods. *Mater. Sci.-Pol* 2021; 39(2): 188–99. doi:10.2478/msp-2021-0017.

[9] Caballero FG., Bhadeshia HKDH, Mawella, KJA, Jones DG, Brown P. Design of novel high strength bainitic steels: Part 2. *Mater Sci Technol.* 2001; 17: 517-522. doi:10.1179/026708301101510357

[10] Sourmail T, Garcia-Mateo C, Caballero FG, Morales-Rivas L, Rementeria R, Kuntz M. Tensile ductility of nanostructured bainitic steels: Influence of retained austenite stability. *Metals* 2017; 7: 31–37. doi:10.3390/met7010031

[11] Sourmail T, Caballero FG, Garcia-Mateo C, Smanio V, Ziegler C, Kuntz M, Elvira R, Leiro A, Vuorinen E, Teeri T. Evaluation of potential of high Si high C steel nanostructured bainite for wear and fatigue applications. *Mater Sci Technol* 2013; 29(10): 1166–1173. doi:10.1179/1743284713Y.0000000242.

[12] Du Y, Wang X, Zhang D, Wang X, Ju C, Jiang B. A superior strength and sliding wear resistance combination of ductile iron with nanobainitic matrix. *J Mater Res Technol* 2021; 11: 1175–1183. doi:10.1016/j.jmrt.2021.01.104.

[13] Rios-Diez, O, Aristiza´bal-Sierra R, Serna-Giraldo C, Eres-Castellanos A, Garcia-Mateo C. Wear behavior of nanostructured carboaustempered cast steels under rolling-sliding conditions. *J Mater Res Technol* 2021; 11: 1343–1355. doi:10.1016/j.jmrt.2021.01.094.

[14] Sukumar G, Senthil PP, Reddy PRS, Singh BB, Ramakrishna B, Kumar KS, Madhu V. Ballistic efficacy of carbide free high strength nano-structured bainitic armour steels. *Def Sci J.* 2023; 73(2): 131–139. doi:10.14429/dsj.73.18634.

[15] Caballero FG, Bhadeshia HKDH, Mawella KJA, Jones DG, Brown P. Very strong low temperature bainite. *Mater Sci Technol* 2002; 18: 279–284. doi:10.1179/026708301225000725.

[16] Garcia-Mateo C, Caballero FG. Design of carbide-free low-temperature ultra high strength bainitic steels. *Int J Mat Res* 2007; 98(2): 137–143. doi:10.3139/146.101440

[17] Garcia-Mateo C, Caballero FG, Sourmail T, Cornide J, Smanio V, Elvira R. Composition Design of nanocrystalline bainitic steels by diffusionless solid reaction. *Met Mater Int.* 2014; 20(3): 405–415. doi:10.1007/s12540-014-3002-9.

[18] Wojtaszek M, Lisiecki Ł, Łukaszek - Sołek A, Korpała G, Zyguła K, Śleboda T, Jabłońska MB, Prahl U. Application of processing maps and numerical modelling for identification of parameters and limitations of hot forging process of 80MnSi8-6 steel. *Arch Civ Mech Eng.* 2023; 23(4): 1–22. doi:10.1007/s43452-023-00783-8.

[19] Sourmai T. Bainite and superbainite in long products and forged applications. *HTM.* 2017; 72(6): 371–378. doi:10.3139/105.110342.

[20] Leiro A, Vuorinen E, Sundin KG, Prakash B. Wear of nano-structured carbide-free bainitic steels under dry rolling-sliding conditions. *Wear.* 2013; 298–299: 42–47. doi:10.1016/j.wear.2012.11.064.

[21] Jabłońska MB, Śmiglewicz A, Niewielski G. The effect of strain rate on the mechanical properties and microstructure of the high-Mn steel after dynamic deformation tests. *Arch Metall Mater.* 2015; 60(2): 577–80. doi:10.1515/amm-2015-017.

[22] Agha A, Abu-Farha F. A Method for Measuring In-Plane Forming Limit Curves Using 2D Digital Image Correlation. *SAE Int J Mater Manf.* 2023; 16(3): 281–291. doi:10.4271/05-16-03-0019.

[23] Szalai S, Csótár H, Kurhan D, Németh A, Sysyn M, Fischer S. Testing of lubricants for dic tests to measure the forming limit diagram of aluminum thin sheet materials. *Infrastructures.* 2023; 8: 1–14. doi:10.3390/infrastructures8020032.

[24] King M, Rahimi S. Optimisation of sample geometry for thermo-mechanical testing of precipitation hardenable nickel-based superalloys with an ETMT machine. *Strain.* 2023; e12458: 1–18. doi:10.1111/str.12458.

[25] Van der Heijde JH, Samad WA. The effect of specimen thickness on the lüders phenomena in aisi 1524 steel alloy: Experimental observations using DIC. *Exp Mech.* 2023; 63: 885–896. doi:10.1007/s11340-023-00951-0.

[26] Champolivier E, Brancherie D, Feissel P, Gaied S, Canourgues J-F. Experimental characterization of forming behavior of 3rd GEN AHSS. IOP Conf. Series: Materials Science and Engineering 2023. 1284, 012077, 1–9. doi:10.1088/1757-899X/1284/1/012077.

[27] He T, Liu L, Makeev A, Shonkwiler B. Characterization of stress-strain behaviour of composites using digital image correlation and finite element analysis. *Compos Struct.* 2016; 140: 84–93. doi:10.1016/j.compstruct.2015.12.018.

[28] Roux E, Bouchard PO. On the interest of using full field measurements in ductile damage model calibration. *Int J Solids Struct* 2015; 72: 50. doi:10.1016/j.ijsolstr.2015.07.011.

[29] Sutton MA, Orteu JJ, Schreier H. Image correlation for shape, motion and deformation measurements: basic concepts, theory and applications. Springer Science & Business Media; 2009. 332 p.

[30] Dumoulin S, Tabourot L, Chappuis C, Vacher P, Arrieux R. Determination of the equivalent stress–equivalent strain relationship of a copper sample under tensile loading. *J Mater Process.* 2003; 133: 79. doi:10.1016/S0924-0136(02)00247-9.

[31] Lisiecka-Graca P, Majta J, Muszka K. Full-field strain measurement and numerical analysis of a microalloyed steel subjected to deformation with strain path change. *Materials.* 2020; 11: 1–17. doi:10.3390/ma1323 5543.

[32] Christiansen P, Hattel JH, Bay N, Martins PAF. Modelling of damage during hot forging of ingots: international conference on modelling and simulation of metallurgical processes in steelmaking. STEELSIM 2013 – The 5th International Conference. 2013.

*Received 2024-01-10*
*Accepted 2024-04-07*